2013 IEEE 10th International Symposium on Biomedical Imaging:
From Nano to Macro
San Francisco, CA, USA, April 7-11, 2013

# BRAIN NETWORK EFFICIENCY AND TOPOLOGY DEPEND ON THE FIBER TRACKING METHOD: 11 TRACTOGRAPHY ALGORITHMS COMPARED IN 536 SUBJECTS

*Liang Zhan[1], Neda Jahanshad[1], Yan Jin[1], Arthur W. Toga[1], Katie L. McMahon[2], Greig I. de Zubicaray[4], Nicholas G. Martin[3], Margaret J. Wright[3,4], Paul M. Thompson[1]*

[1] Imaging Genetics Center, Laboratory of Neuro Imaging, UCLA School of Medicine, Los Angeles, CA, USA
[2]Center for Advanced Imaging, Univ. of Queensland, Brisbane, Australia
[3]Queensland Institute of Medical Research, Brisbane, Australia
[4]School of Psychology, University of Queensland, Brisbane, Australia

## ABSTRACT

As connectivity analyses become more popular, claims are often made about how the brain's anatomical networks depend on age, sex, or disease. It is unclear how results depend on tractography methods used to compute fiber networks. We applied 11 tractography methods to high angular resolution diffusion images of the brain (4-Tesla 105-gradient HARDI) from 536 healthy young adults. We parcellated 70 cortical regions, yielding 70x70 connectivity matrices, encoding fiber density. We computed popular graph theory metrics, including network efficiency, and characteristic path lengths. Both metrics were robust to the number of spherical harmonics used to model diffusion ($4^{th}$-$8^{th}$ order). Age effects were detected only for networks computed with the probabilistic Hough transform method, which excludes smaller fibers. Sex and total brain volume affected networks measured with deterministic, tensor-based fiber tracking but not with the Hough method. Each tractography method includes different fibers, which affects inferences made about the reconstructed networks.

***Index Terms***— Anatomical connectivity, tractography, diffusion imaging, networks, brain, efficiency, random effects analysis

## 1. INTRODUCTION

Graph theory and network analyses are increasingly popular for studying brain connectivity based on neuroimaging data. If the results are reliable, they offer novel insights into the higher-level organization of brain networks and their topological properties in health and disease. Recently, we showed that networks computed from diffusion MRI depend on the spatial and angular resolution of the scans, and the scanner field strength [1, 2]. In addition, remarkably little is known about how stable the network properties are to differences in the fiber tracking methods used to recover them. Tractography methods use numerous diffusion models and tracking principles. Two major approaches are prevalent: deterministic and probabilistic. Deterministic methods, such as fiber assignment by continuous tracking (FACT) [3], are simple and fast. If the diffusion orientation density function (ODF) at a voxel has multiple peaks or dominant directions, FACT follows the closest one (that subtends the smallest angle) to the incoming direction of propagation. Probabilistic algorithms include the whole-brain Hough transform method, which fits vast numbers of polynomial curves through fields of ODFs [4]. This requires long computation time but yields fewer false positive fibers. To understand how these choices affect downstream measures that rely on them, we ran 11 tractography methods on high-angular resolution diffusion imaging (HARDI) data from a large cohort of 536 young adults. Using cortical parcellations from co-registered anatomical MRI, we computed connectivity and network measures from the fiber density matrices. Our goal was to see which graph theoretic metrics were most and least stable to the choice of fiber tracking method, and which statistical predictors of network parameters (if any) were robust to the methods employed.

## 2. METHODS

### 2.1. Subject demographic and 4-Tesla HARDI scans

3D T1-weighted anatomical brain MRI scans and diffusion-weighted scans (DWI) were acquired from 536 healthy young adults (from 334 families, age: 23.46 ± 2.70 years, 346 women) on a 4T Bruker Medspec MRI scanner. T1-weighted images were acquired with an inversion recovery rapid gradient echo sequence, with TI/TR/TE= 700/1500/3.35 ms; flip angle, 8°; slice thickness, 0.9 mm). DW-MRIs were also acquired using single-shot echo planar imaging with a twice-refocused spin echo sequence to reduce eddy-current induced distortions. Acquisition parameters were: 23 cm FOV, TE/TR 92.3/8250 ms. 105 images were acquired per subject: 11 with no diffusion sensitization (i.e., T2-weighted $b_0$ images) and 94 diffusion-weighted (DW) images ($b$=1159 s/mm$^2$) with gradient directions evenly distributed on the hemisphere. Total scan time was 14.5 minutes.

### 2.2. Whole-brain tractography

Non-brain regions were automatically removed from each T1-weighted image, and from a $b_0$ image from the DWI dataset, using *bet* function in FSL (http://fsl.fmrib.ox.ac.uk). A neuroanatomical expert manually refined all brain extractions. We corrected eddy current distortion in DWI scans using FSL's *eddy_correct* function. All T1-weighted scans were linearly aligned using FSL (with 9 DOF) to a common space. For each subject, the 11 eddy-corrected $b_0$ images were averaged, linearly aligned to the corresponding T1 image and elastically registered to the structural scan using a mutual information cost function to compensate for EPI-induced susceptibility artifacts. The resultant deformation field was applied to the other DWIs. Based on these registered DWIs, whole-brain tractography was conducted with a wide variety of deterministic and probabilistic tracking algorithms that used tensor or full ODF-based models of diffusion. Using a tensor-based model, we performed deterministic fiber tracking with FACT and variants of FACT including the 2nd-order Runge-Kutta [5], tensorline [6] and interpolated streamline methods [7]. With the ODF model, we performed deterministic fiber tracking using modified FACT [3], the 2nd-order Runge-Kutta method, and a Hough transform global probabilistic approach [4]. **Table 1** lists all 11 tractography methods assessed; clearly this is just a representative selection, other variants will be of future interest.

**Table 1. Tractography methods evaluated**. 1-10 are deterministic fiber tracking approaches. Methods 5-10 use a *q*-ball derived ODF with a 4th, 6th and 8th order spherical harmonic (SH) basis [8]. The 11th method is probabilistic tracking approach based on the 4th SH CSA ODF [9]. RK means 2nd-order Runge-Kutta, TL means tensorline, and SL means interpolated streamline.

| | | | |
|---|---|---|---|
| 1 | Tensor-FACT | 5 | 4th-ODF- RK |
| 2 | Tensor-RK | 6 | 4th-ODF- FACT |
| 3 | Tensor-TL | 7 | 6th-ODF- RK |
| 4 | Tensor-SL | 8 | 6th-ODF- FACT |
| 9 | 8th-ODF- RK | 10 | 8h-ODF- FACT |
| 11 | 4th-ODF-Hough | | |

All deterministic tracking approaches were conducted with the Diffusion Toolkit (http://trackvis.org/dtk/). Fiber tracking was restricted to regions where fractional anisotropy (FA) ≥ 0.2 to avoid gray matter and cerebrospinal fluid; fiber paths were stopped if the fiber direction encountered a sharp turn (with a critical angle threshold ≥ 30°). Sharp "right-angle" turns may be biologically possible in some cases [10], but allowing right-angle turns in tractography would create large numbers of false positive pathways at fiber crossings. Hough tractography (#11) was conducted with code provided by the authors of [4], by probabilistically seeding voxels with a prior probability based on the FA value. All curves passing through a seed point receive a score estimating the probability of the existence of the fiber, computed from the ODFs. Then a Hough transform voting process was adopted to determine the best fitting curves through each point.

After whole-brain tractography, elastic deformations obtained from the EPI distortion correction, mapping the average $b_0$ image to the T1-weighted image, were applied to all tracts' 3D coordinates to accurately align the anatomy. All fibers shorter than 10mm were filtered out as these were much more likely to be false positive fibers.

### 2.3. Computing the Brain Connectivity Network

35 cortical regions of interest (ROI) per hemisphere, listed in [11], were automatically extracted from all aligned T1 scans with FreeSurfer (http://surfer.nmr.mgh.harvard.edu). T1-weighted images and cortical models were then aligned to the original T1 input image space and down-sampled to the space of the DWIs, using nearest neighbor interpolation (to avoid intermixing of labels). To ensure tracts would intersect cortical labeled boundaries, we dilated labels with an isotropic box kernel of size 5×5×5 voxels. For each ROI pair, the number of fibers connecting them was determined from the tractography. A fiber was considered to connect two ROIs if it intersected both ROIs. This process was repeated for all ROI pairs, to compute a 70x70 whole brain fiber connectivity matrix. This matrix is symmetric, by definition, and has a zero diagonal (no self-connections). **Figure 1** shows a flowchart of steps used to compute brain connectivity matrices.

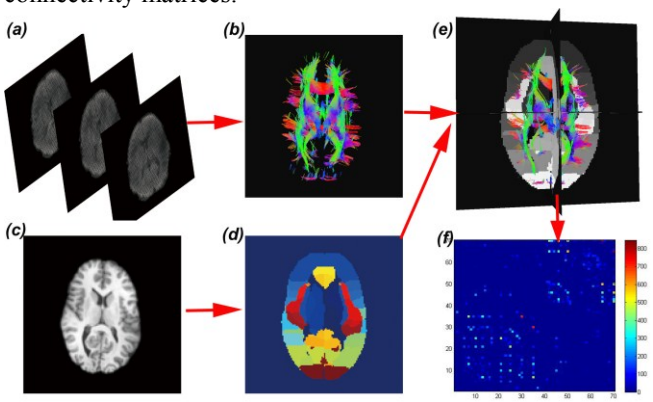


**Figure 1. Flowchart of steps to compute brain connectivity**. Diffusion weighted images (a) are used to perform whole-brain tractography (b); in parallel, the standard T1-weighted anatomical MRI from the same subject (c) is parcellated to define cortical ROIs (d); by counting the number of detected fibers connecting each pair of ROIs (e), and expressing them as a proportion of all fibers recovered in the entire brain, we created an anatomical connectivity matrix (f), for each subject in the study, and for each tractography method listed in **Table 1**.

### 2.4. Graph theoretical analysis and linear mixed model

We used the Brain Connectivity Toolbox (http://www.brain-connectivity-toolbox.net/) [12] to compute two standard graph theory measures, Characteristic Path Length (CPL) and Global Efficiency (GLOB), for each 70x70 brain

connectivity matrix across all 536 subjects and all 11 tractography methods (**Table 1)**. CPL measures network integration by averaging the shortest path lengths between all pairs of nodes. GLOB is the sum of the inverses of the shortest distances between each pair of nodes. Lower GLOB values and longer CPL values jointly indicate less efficient networks although whether or not they are functionally less efficient is conjectural without relevant functional data. We adopted weighted (not binarized) networks to calculate these two measures to reduce bias in determining the sparsity to binarize a network. Formulae for both measures are in [12].

General linear mixed modeling (GLMM) was used to estimate statistical effects of age, sex and total brain volume (TBV) on these two graph theory measures:

$$Y \sim A + \beta_{age} Age + \beta_{sex} Sex + \beta_{TBV} TBV + \alpha \quad \text{(Eq. 1)}$$

Here $Y$ is one of the two graph theory measures, $A$ is a constant for each regression model, the $\beta$s are the covariate regression coefficients, and α is a coefficient that accounts for random effects, which were used to account for family relatedness in this study. We modeled the other variables (age, sex and TBV) as fixed effects.

## 3. RESULTS AND DISCUSSION

### 3.1. Effect of tractography method on networks

**Figure 2** shows the CPL and GLOB network measures derived with the 11 different tractography methods in **Table 1**. Clearly, each network measure depends on the tractography method used. Encouragingly, we did not detect any effect of the order of the spherical harmonic series used for the diffusion ODF: both network measures were consistent across the 5th, 7th and 9th methods or 6th, 8th and 10th methods, which use same tracking method but with a different SH order. The SH order influences the ODF sharpness and geometry but does not greatly affect the peak positions on the ODF, perhaps accounting for the consistency of these network properties.

### 3.2. Predictors of Network Properties

We also assessed whether age, sex, and TBV consistently predicted the network properties, and they did not. **Figure 3** shows *p*-values from the GLMMs used to predict each of the two network properties (**Eq. 1**). Only the whole-brain probabilistic approach (the 11th method), picked up an Age effect (*blue* *) on both network CPL and efficiency [13]. To avoid inflating the false positive rate due to running multiple algorithms, we set the Bonferroni corrected significance level to 0.05/22 (two measures and 11 methods). Visual comparison of fibers from all methods suggested that the probabilistic approach tends to capture longer anatomically-recognizable fiber pathways, but far fewer very short fibers that could be false positives. Although we have no ground truth, it could be that the age effect is relatively strong on these "large" fibers, but not so consistent on the smaller fibers, which the deterministic algorithms tend to pick up in larger numbers.

The Sex effects were also surprising. The network efficiency, GLOB, was influenced by Sex when deterministic models were used to track fibers (**Fig. 3**, top panel, A), but not otherwise. CPL was significantly affected by Sex if tensor-derived deterministic tracking approaches were used (Region A). No Sex (or TBV) effect was picked up with the Hough method, but the Age effect was found. The most reasonable explanation is that the tractography methods do pick up different classes of fibers, which are then included in the networks. For instance, tensor-based methods may fail more often in regions with crossing or mixing fibers. Covariates such as Age and Sex may affect some classes of fibers but not others, so the conclusions may depend on the method used.

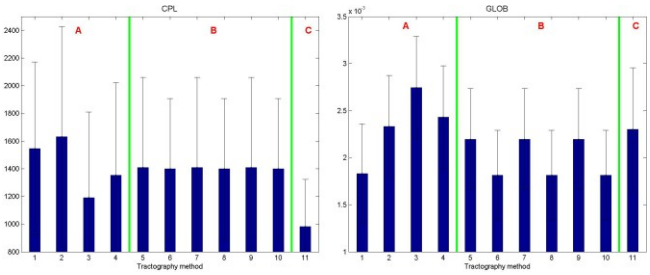


**Figure 2**. **Two popular brain network measures (CPL, *left*, and GLOB, *right*) are derived from 11 different tractography methods.** The *x*-axis shows the tractography method index (from **Table 1**) and the *y*-axis shows the mean network measure across 536 subjects. The error bar shows the standard deviation of the mean network measure. Two *green lines* divide the algorithms into 3 categories: (A) tensor-derived deterministic tracking methods; (B) *q*-ball ODF-derived deterministic tracking methods; (C) probabilistic tracking with Hough transform and fields of CSA-ODFs.

## 4. CONCLUSION

In this study, we compared 11 different deterministic and probabilistic fiber tracking methods (**Table 1**). We set out to find out if different tractography methods tend to detect the same effects, when applied to a large cohort of 536 adults. We studied two popular network measures – efficiency and characteristic path length. Whether or not these measures depended on the age, sex or brain volume of the subject depended on the algorithm used. Clearly, the methods extract different classes of fibers from the images. Age effects were found on the networks from the Hough method only, which tends to extract the longer fibers and suppress smaller ones. Although some methods may make more errors overall, there was no one algorithm that provided universally greater or 'better' effect sizes when studying what affects the networks. Other effects, of Sex and TBV for example, were only picked up with the tensor-based tracking methods, which are known make more errors in

regions where fibers cross. Even so, despite the differences arising from using different methods, some methodological parameters, such as the order of the spherical harmonic series used to represent directional diffusion, did not strongly affect the network properties.

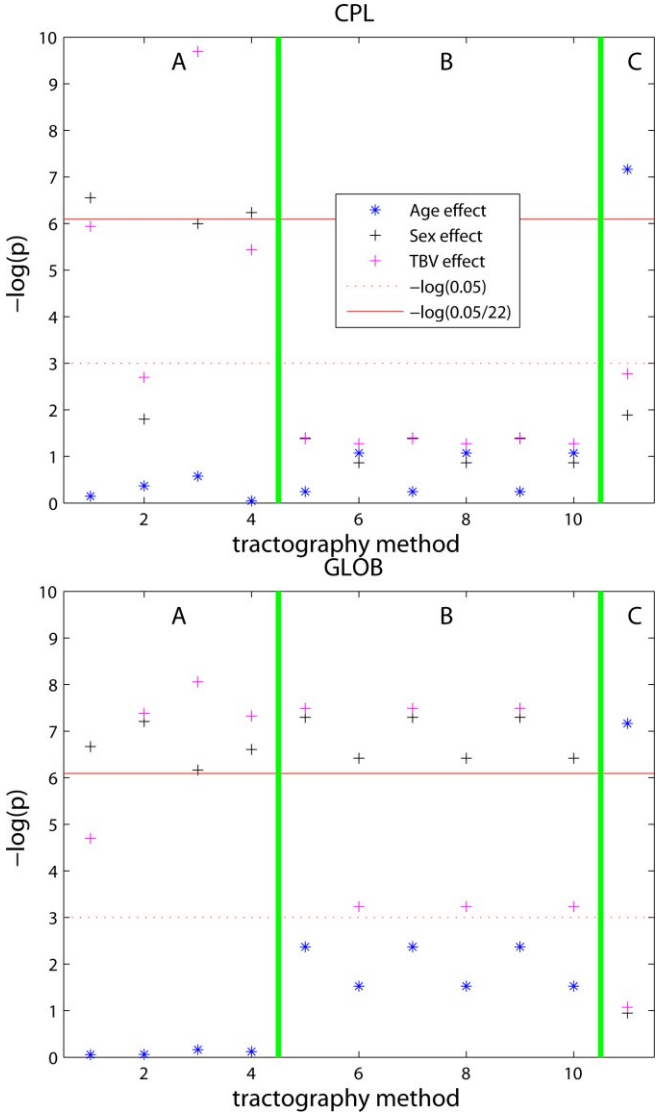


**Figure 3. Age/Sex/TBV effects on graph theory measures of anatomical network properties in the brain.** The *x*-axis indicates the tractography method, corresponding to the 11 methods listed in **Table 1.** The *y*-axis shows the GLMM significance ***P*** (on a –log(*p*) scale). On the Hough transform probabilistic approach (the 11th method) picked up an Age effect on the networks (*blue* *); this effect was strong enough to easily survive Bonferroni correction for multiple statistical tests (*alpha*<0.05/22). Network efficiency, GLOB, was significantly affected by TBV and Sex for most deterministic tracking approaches, while CPL was significantly affected by Sex only when networks were computed with tensor-derived deterministic tracking (see part A of the figure).

These results suggest great caution when making assertions about what factors affect anatomical networks in the brain. Although the brain's network appears to be a stable and well-defined concept, the fibers included in it and all downstream assertions depend on the methods used. As such, it is unlikely that effects on the human connectome will be replicated across cohorts without great care in harmonizing either the acquisition or analysis. With this in mind, several international efforts are underway to make DTI-derived measures less sensitive to the methods used to acquire and analyze the data, to allow large scale data pooling (such as ENIGMA-DTI; http://enigma.loni.ucla.edu/ongoing/dti-working-group/). In determining factors that affect fiber connectivity, one safeguard would be to run all available tractography methods on DTI datasets to test the stability of findings. Findings from different studies may be inconsistent due to the differential inclusion of different components in the networks. As network metrics depend on the scanner field strength, spatial and angular resolution of the scans, and the parcellation scheme used, future work will attempt to define network metrics more robust to the methods used.

## 5. REFERENCES


[1] Zhan et al., How do Spatial and Angular resolution affect brain connectivity maps from Diffusion MRI? **Proc IEEE Int Symp Biomed Imaging.** 2012:1-6.

[2] Zhan et al., MR Field Strength Effects on Diffusion Measures and Brain Connectivity Network. Revision submitted to **Brain Connectivity**, 2012.

[3] Mori et al. Three-dimensional tracking of axonal projections in the brain by magnetic resonance imaging. **Ann. Neurol**. 45(2):265-9, 1999.

[4] Aganj et al., A Hough transform global probabilistic approach to multiple-subject diffusion MRI tractography. **Med. Image Analysis**, 15:414-425, 2011.

[5] Basser et al. In vivo fiber tractography using DT-MRI data. **Magn. Reson. Med**. 44(4):625-32, 2000.

[6] Lazar et al., White matter tractography using diffusion tensor deflection. **Hum. Brain Mapp**. 18(4):306-21, 2003.

[7] Conturo et al., Tracking neuronal fiber pathways in the living human brain. **PNAS,** 96:10422-27, 1999.

[8] Hess et al., Q-ball reconstruction of multimodal fiber orientations using the spherical harmonic basis. **Magn. Reson. Med.** 56(1):104-17, 2006.

[9] Aganj et al., Reconstruction of the orientation distribution function in single and multiple shell q-ball imaging within constant solid angle. **Magn. Reson. Med.** 64(2):554–66, 2010.

[10] Wedeen et al., The Geometric Structure of the Brain Fiber Pathways. **Science**, 335(6076): 1628-34, 2012

[11] Desikan et al., An automated labeling system for subdividing the human cerebral cortex on MRI scans into gyral based regions of interest. **NeuroImage**, 31:968-980, 2006.

[12] Rubinov M, Sporns O. Complex network measures of brain connectivity: Uses and interpretations. **NeuroImage**, 52(3): 1059-69, 2010.

[13] Dennis et al., Development of Brain Structural Connectivity between Ages 12 and 30: A 4-Tesla HARDI Study in 439 Adolescents and Adults. **NeuroImage**, 64(1):671-84, 2912.